A Time Domain Model of GPR Antenna Radiation Pattern

Fedor Edemsky, Alexei Popov, and Sergey Zapunidi

Abstract—**The problem of transient EM radiation by a linear current source placed on the ground-air interface is analytically studied. We derive a self-modeling exact solution for the interfacial Green function. The spatio-temporal radiation pattern is constructed by means of the Duhamel integral. An inverse problem of antenna current reconstruction from the measured waveform of direct surface wave is solved analytically. An example of real GPR data deconvolution is given.**

Keywords—**Subsurface sensing, Ground Penetrating Radar (GPR), electromagnetic pulse radiation, ground-air interface, time-domain Green function, spatio-temporal radiation pattern, inverse problem, deconvolution.**

I. INTRODUCTION

THE problem of electromagnetic radiation from a horizontal electric dipole placed on the earth's surface has been studied in a number of classical works, e.g. [1], [2] related to the issues of radio communication. Attention was paid mainly to the laws of harmonic wave propagation along the ground-air interface.

Radiation patterns of a point dipole and of an infinitely long linear antenna have been derived in [3]. An exact solution was found using Fourier transform in a complex plane. Derivation of the far-field radiation pattern, lateral wave and the wave field in the intermediate regions requires sophisticated asymptotic and numerical approaches [3], [4]. The problem of wide-band pulsed radiation is much less studied. An analytical approach, based on the Smirnov-Sobolev concept of functionally-invariant solution [5] has been used in [6] to study the lateral ("head") wave which plays an important role in seismic prospecting.

Nowadays, a renewed interest to the problem of EM radiation by antennas lying on the interface between two dielectric media is motivated by the needs of subsurface sensing (ground penetrating radar, GPR) and microelectronics. Direct numerical schemes for solving Maxwell's equations are commonly used to calculate the propagation of realistic ultrawideband (UWB) pulses [7]. As this approach involves a great amount of numerical calculations it is suitable only for idealized model problems or for a thorough post-processing of a few selected GPR profiles. In practice, the radiation pattern of a monopulse GPR antenna is usually estimated on the basis of the harmonic wave theory and the centre frequency concept. This leads to the loss of information contained in the waveform of the received GPR signal.

F. Edemsky, A. Popov, and S. Zapunidi are with Institute of Terrestrial Magnetism, Ionosphere and Radiowave Propagation, Russia, Troitsk (Moscow region) (e-mails: edem.teo@gmail.com, popov@izmiran.ru, zapunidy@gmail.com).

Of course, in virtue of the superposition principle, the classical solution of the monochromatic wave radiation problem can be used for the calculation of a UWB antenna by Fourier transform. However, straightforward problem treatment in time domain looks more promising. Following the Smirnov-Sobolev approach, we derive an elementary solution of the time-dependent 2D wave equation that substantially simplifies calculations and clarifies the physical mechanisms of the wave field formation.

By convolving the obtained time-domain Green function with a given current pulse form, we simulate realistic spatiotemporal radiation patterns of resistively-loaded GPR dipole antennas. Next, the inverse problem of the antenna current reconstruction from the electric field measured at the ground-air interface is solved in a closed form. Finally, an example of realistic GPR profile deconvolution is given.

II. EXPLICIT SOLUTION OF THE WAVE EQUATION

Consider a model problem of transient radiation from an infinite line current source stretched along y-axis on the $z = 0$ plane being the interface between two uniform dielectric half-spaces: $z > 0$ ("ground") and $z < 0$ ("air"). Neglecting the conductivity effects, we characterize "ground" by a single parameter $n = \sqrt{\epsilon_r} > 1$ (refraction index), whereas the "air" half-space has $n_0 = 1$. In this essentially 2D model, Maxwell's equations are reduced to a scalar wave equation governing the horizontal component of the electrical field $E_y = E(x, z, t)$ excited by a pulsed current source $J(t)$ at the origin $(x = 0, z = 0)$:

$$\frac{\partial^2 E}{\partial x^2} + \frac{\partial^2 E}{\partial z^2} - \frac{n^2}{c^2}\frac{\partial^2 E}{\partial t^2} = \frac{4\pi}{c^2}\delta(x)\delta(z)\frac{dJ}{dt} \quad (1)$$

The heuristic considerations leading to the proper choice of the sought solution form are as follows. Consider a line antenna in free space with $n_0 = 1$ excited by a unit current step $J(t) = \Theta(t)$ (Heaviside function). In contrast to the harmonic wave field depending on the wavelength $\lambda = \dfrac{2\pi c}{\omega}$, in our case the only parameter of the dimension of length is the distance from the point source: $r = \sqrt{x^2 + z^2}$. In this case, the corresponding solution of the equation (1) is the pulsed Green function [8]:

$$E_0(r, t) = (s^2 - r^2)_+^{-1/2} = \begin{cases} \dfrac{1}{\sqrt{s^2 - r^2}}, & s = ct > r \\ 0, & s < r \end{cases} \quad (2)$$

(here and below $s = ct$). Convolution of this function with the antenna pulse form (Duhamel integral) represents transient

radiation generated by an arbitrary current $J(t)$:

$$E_0(r,t) = (s^2 - r^2)_+^{-1/2} = \begin{cases} \dfrac{1}{\sqrt{s^2 - r^2}}, & s = ct > r \\ 0, & s < r \end{cases} \quad (3)$$

Obviously, the Green function can be represented as a function of dimensionless parameter $\tau = \dfrac{s}{r}$, with an additional factor $\dfrac{1}{r}$ taking into account geometrical divergence of the emitted wave:

$$G_0(r,t) = \frac{1}{r} V_0(\tau) \quad (4)$$

where $V_0(\tau) = (\tau^2 - 1)_+^{-1/2}$. We can expect that in the case of a line source lying at the interface between two uniform media the Green function has a similar form:

$$G(r,\theta,t) = \frac{1}{r} V(\tau,\theta) \quad (5)$$

where just the dependence on the angular variable $\theta = \text{atan}\frac{x}{z}$ is added to take into account the influence of the interface on the radiation pattern. Substitution of the expression (5) into (1) yields a new equation

$$(\tau^2 - n^2)\frac{\partial^2 V}{\partial \tau^2} + 3\tau\frac{\partial V}{\partial \tau} + \frac{\partial^2 V}{\partial \theta^2} + V = 0 \quad (6)$$

containing only dimensionless variables and describing the sought self-modeling solution $V(\tau,\theta)$. Following the method of [5], we look for a solution in the form of generalized cylindrical waves:

$$V(\tau,\theta) = \text{Re}\left(\frac{1}{\sqrt{\tau^2 - n^2}} B\left(|\theta| + i\text{Arcosh}\frac{\tau}{n}\right)\right) \quad (7)$$

in the subsurface medium $z > 0$ $\left(|\theta| < \dfrac{\pi}{2}\right)$, and

$$V(\tau,\theta) = \text{Re}\left(\frac{1}{\sqrt{\tau^2 - 1}} A(\pi - |\theta| + i\text{Arcosh}\tau)\right) \quad (8)$$

in free space $z > 0$ $\left(|\theta| < \dfrac{\pi}{2}\right)$.

Here, $A(\alpha)$ and $B(\beta)$ are analytic functions, arbitrary so far, regular for $\tau > n$, behind the slow wave front, where the total wave field has no jumps. These functions can be found from the conditions of smooth matching the tangent components of EM field, that reduce to the continuity of V and $\dfrac{\partial V}{\partial \theta}$ at $|\theta| = \dfrac{\pi}{2}$. Explicitly,

$$\begin{cases} \dfrac{1}{\sqrt{\tau^2 - 1}} A\left(\dfrac{\pi}{2} + i\text{Arcosh}\tau\right) = \dfrac{1}{\sqrt{\tau^2 - n^2}} B\left(\dfrac{\pi}{2} + i\text{Arcosh}\dfrac{\tau}{n}\right) \\ -\dfrac{1}{\sqrt{\tau^2 - 1}} A'\left(\dfrac{\pi}{2} + i\text{Arcosh}\tau\right) = \dfrac{1}{\sqrt{\tau^2 - n^2}} B'\left(\dfrac{\pi}{2} + i\text{Arcosh}\dfrac{\tau}{n}\right) \end{cases} \quad (9)$$

Denoting

$$\alpha = \frac{\pi}{2} + i\text{Arch}\tau, \quad \beta = \frac{\pi}{2} + i\text{Arch}\frac{\tau}{n} \quad (10)$$

and eliminating from (10) the variable τ, we obtain a function $\beta(\alpha)$ determined by Snell's law

$$n\sin\beta = \sin\alpha, \quad \beta'(\alpha) = \frac{\cos\alpha}{n\cos\beta} \quad (11)$$

After introducing a new unknown function $B^\%(\alpha) = B[\beta(\alpha)]$, the second equation (9) can be integrated to $A^+(\alpha) + B^+(\alpha) = K = \text{Const}$, and the first one yields an explicit solution

$$\begin{cases} A(\alpha) = \dfrac{\cos\alpha}{\cos\alpha + n\cos\beta} \\ B(\beta) \equiv \widetilde{B}(\alpha) = \dfrac{n\cos\beta}{\cos\alpha + n\cos\beta} \end{cases} \quad (12)$$

for $\tau > n$. At lower dimensionless times, for $1 < \tau < n$, the solution is found by analytic continuation.

III. NUMERICAL IMPLEMENTATION AND CONSEQUENCES

The obtained solution describes all the wave field singularities predicted by geometrical optics and physical theory of diffraction (see, e.g. [3]–[6], [8]): sharp circular wave fronts $\tau = 1$ and $\tau = n$ n in the corresponding half-spaces and a weak singularity at the plane lateral wave front $|\theta| = \psi + \eta$, where $\psi = \arccos\frac{\tau}{n}$, $\eta = \arccos\frac{1}{n}$. A graphical representation of the function $V(\tau,\theta)$ for a fixed t ("snapshot") is given by Fig.1.

Transient Green function (5) and Duhamel integral (3) make an efficient tool of deriving the global spatio-temporal radiation pattern for an arbitrary current pulse form. As an illustration, in Fig.2 a polar plot of $E(r,\theta,s)$ is depicted as a function of time (actually, $s = ct$) and observation angle θ for a fixed radius $t = \text{Const}$ and a one-period sinusoidal current pulse form – see Fig. 5 (a).

In order to relate our solution to the commonly referred results for the harmonic waves we trace the formation of the far field radiation pattern of the wave generated by a few periods of sinusoidal current pulse – see Fig.3. One can see that the peak amplitude values tend to the far-field pattern with sharp edges at the critical total reflection angles $|\theta| = \eta$ calculated in [4] but quite slowly – at unrealistic for GPR application distances of many decameters.
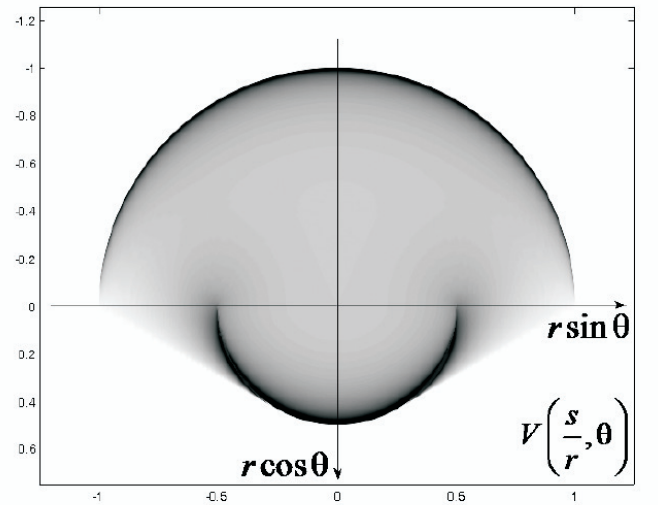

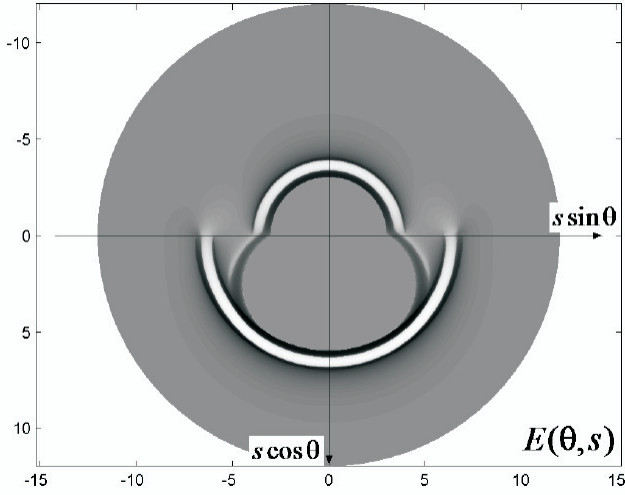Fig. 1.   Snapshot of the self-modeling solution $V(\tau,\theta)$.

Fig. 2.   Spatio-temporal radiation pattern for a one-period sinusoidal current pulse form (logarithmic scale).

Fig. 4.   Sounding pulse form for a one-period sinusoidal current pulse related to the direction of propagation. (1) upwards, (2) along the interface, (3) in the lateral wave sector, (4) downwards.

The most important feature of the spatio-temporal radiation pattern is dependence of the probing pulse waveform on the radiation angle. Some characteristic bearings are depicted in Fig.4. While the pulses radiated vertically upwards and downwards, marked by numbers 1 and 4, are quite similar, signals propagating obliquely in the sector $\eta < |\theta| < \pi/2$, represented by the curve 3, have a pronounced precursor due to the lateral "Cherenkov" wave. Of special interest is the signal propagating along the ground-air interface (curve 2). It consists of two pulses of opposite polarity, propagating with different velocities, and has a waveform distinct from the other bearings.
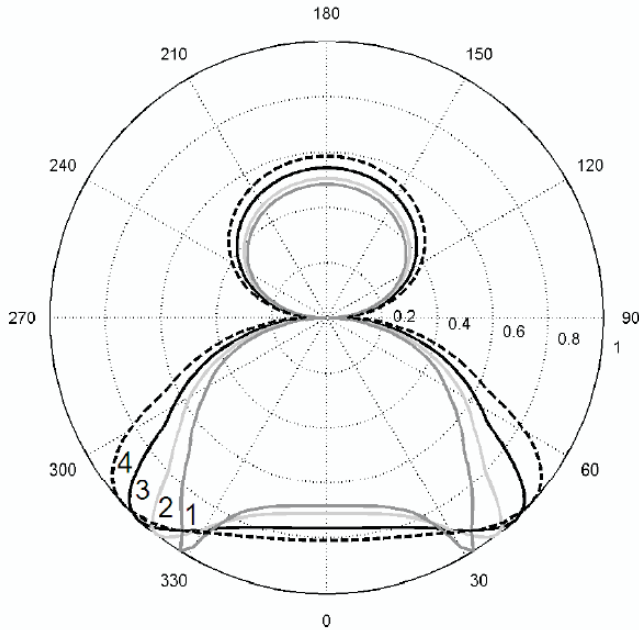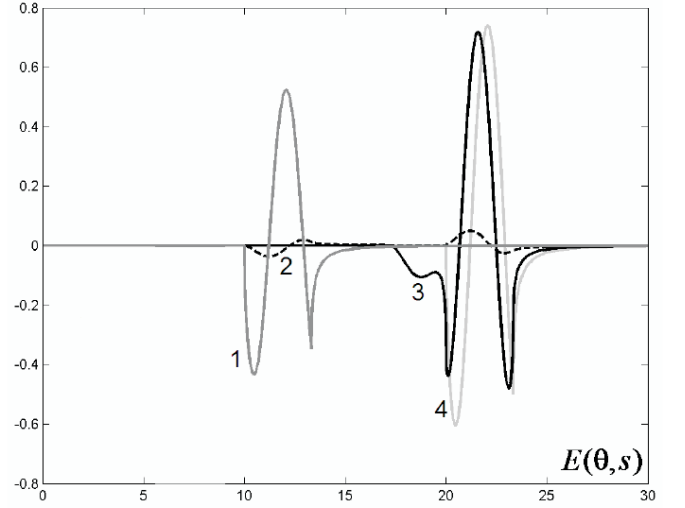
IV.   INITIAL PULSE RECONSTRUCTION BY THE INTERFACE SIGNAL

In modern ground penetrating radars recording full received signal waveform, the interface signal produces characteristic stripes in the upper part of the GPR scan – see Fig.6 (a). Common practice is just to use them as a reference point for the time count. However, this direct signal contains information both on the ground velocity $v = \dfrac{c}{n}$ and the antenna current pulse form $J(t)$. A stable numerical algorithm for antenna current reconstruction has been developed in [9].

In what follows, we derive a closed-form solution of this inverse problem and give a numerical example. The self-modeling solution (7)-(8) takes the simplest form on the ground-air interface $\theta = \dfrac{\pi}{2}$:

$$V\left(\tau, \frac{\pi}{2}\right) = \mathrm{Re}\left(\frac{2}{\sqrt{\tau^2 - 1} + \sqrt{\tau^2 - n^2}}\right) =$$

$$= \frac{2}{n^2 - 1}\left(\sqrt{\tau^2 - 1}_+ - \sqrt{\tau^2 - n^2}_+\right) \qquad (13)$$

After substitution into the Duhamel integral, the latter takes the following form

$$E\left(r, \frac{\pi}{2}, s\right) = -\frac{4}{cr(n^2 - 1)}\left[\int_1^\infty J(s - r\xi)\frac{\xi d\xi}{\sqrt{\xi^2 - 1}} -\right.$$

$$\left. - \int_n^\infty J(s - r\xi)\frac{\xi d\xi}{\sqrt{\xi^2 - n^2}}\right] \qquad (14)$$

If the electric field on the interface $E_0(s) = E\left(r, \dfrac{\pi}{2}, s\right)$ is known, this formula becomes an integral equation for the primary current $J(s)$. It can be solved by Laplace transform.

Fig. 3.   Peak radiation pattern. The space between transmitter and receiver: (1) 200 m, (2) 12 m, (3) 4 m, (4) 2 m.
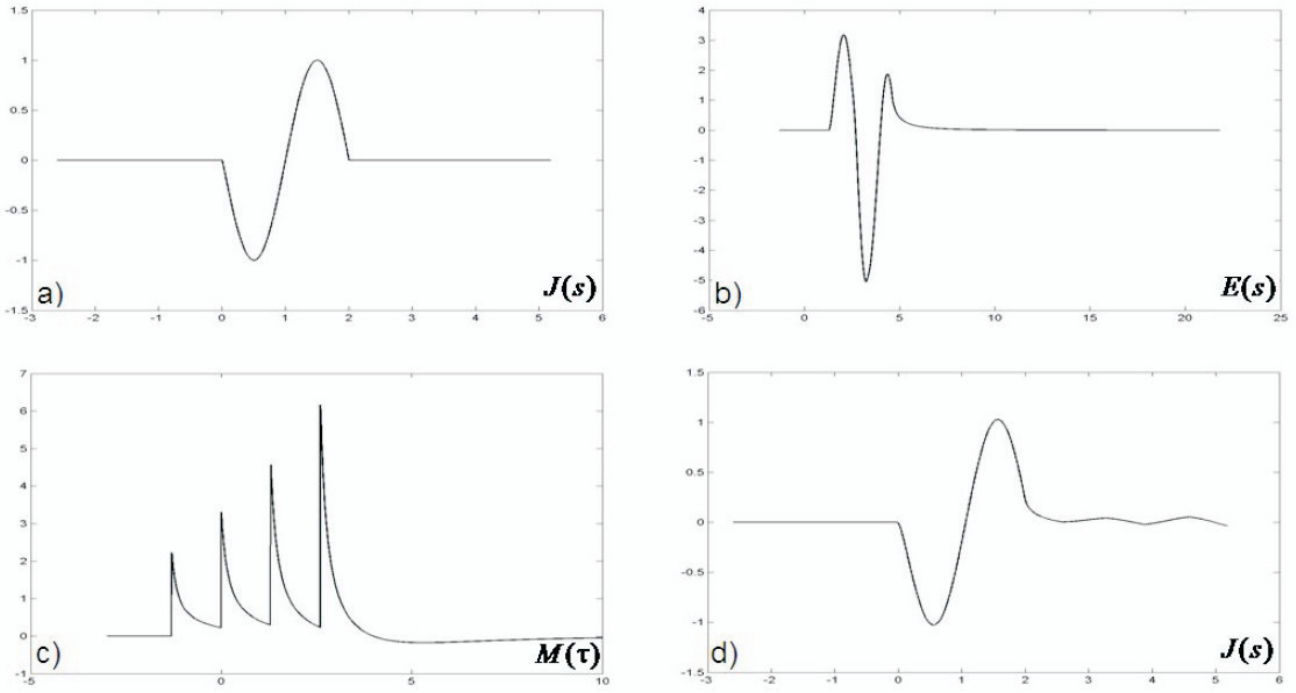
Fig. 5. Model example of the pulse current form reconstruction using the signal that propagates along the interface. Relative permittivity of the subsurface medium $\epsilon = 4$, antenna separation $R = 1.3$m. a) Initial current pulse form, b) Signal along the interface, c) Sum of the first four terms of series for $M(\tau)$, d) Reconstructed pulse form.

Making use of the Macdonald function integral representation [10] we obtain: $E_0^{\%}(p) = J^{\%}(p)G_0^{\%}(p)$, where

$$G_0^{\%}(p) = -\frac{2}{\pi i c r(n^2-1)}[K_1(pr) - nK_1(npr)] \qquad (15)$$

Functions $G_0^{\%}(p)$ and $J^{\%}(p)$ are Laplace images of the Green function boundary value $G_0(r,t) = \frac{1}{r}V\left(\tau, \frac{\pi}{2}\right)$ and of the current pulse form $J(s)$, respectively. Expressing $J^{\%}(p)$ as a ratio of $E_0^{\%}(p)$ and $G_0^{\%}(p)$ and calculating the inverse Laplace transform we obtain a convolution integral

$$J(s) = -\frac{cr(n^2-1)}{4}\frac{d}{ds}\int_0^\infty E_0(\xi)M\left(\frac{s-\xi}{r}\right)d\xi \qquad (16)$$

whose kernel $M(\tau)$ is a new special function

$$M(\tau) = \frac{1}{2\pi i}\int_{\gamma-i\infty}^{\gamma+i\infty} e^{\tau w}\frac{dw}{w[K_1(w) - nK_1(nw)]} \qquad (17)$$

Direct calculation of the complex integral (17) presents certain difficulties due to multiple poles of the integrand and emerging quasi-periodic numerical errors. However, by representing the integrand as a sum of a geometrical series

$$\frac{1}{K_1(w) - nK_1(nw)} = \frac{1}{K_1(w)} + \frac{nK_1(nw)}{K_1^2(w)} + \frac{n^2K_1^2(nw)}{K_1^3(w)} + \cdots \qquad (18)$$

we come to an absolutely converging series

$$M(\tau) = \sum_{\mu=0}^\infty M_\mu(\tau), \text{ where functions}$$

$$M_\mu(\tau) = \frac{1}{2\pi i}\int_{\widetilde{A}} e^{\tau w}\frac{n^\mu K_1^\mu(nw)}{K_1^{\mu+1}(w)}\frac{dw}{w} \qquad (19)$$

can be reduced to easily evaluated integrals. For any fixed value of τ the series contains a finite number of terms, because – as follows from the asymptotic behavior of the Macdonald function, $M_\mu(\tau) = 0$ for $\tau < \mu(n-1) - 1$. For most GPR problems, it is enough to keep 2-3 terms of the series.

The behavior of the convolution kernel $M(\tau)$ and a model numerical example of antenna current reconstruction are depicted in Fig. 5. Obviously, the main reason of the inverse problem instability is the growing amplitude of successive peaks of the $M(\tau)$ function. Nevertheless, by using a priori information on the primary current duration and the least square method, it is possible to develop a stable numerical procedure.

V. DECONVOLUTION OF COMMON-OFFSET DATA

The obtained inverse problem solution allows one to improve the resolution of subsurface object by deconvolution of the primary GPR data from the reconstructed antenna current pulse form. Basically, such a procedure removes the fringes caused by the oscillations of the primary current pulse, although measurement errors and numerical ill-conditionedness may outweigh the improvement. A more stable procedure can be used that skips the step of antenna current reconstruction. As the Laplace images of the actual radiation pattern $E(r, \theta, t)$
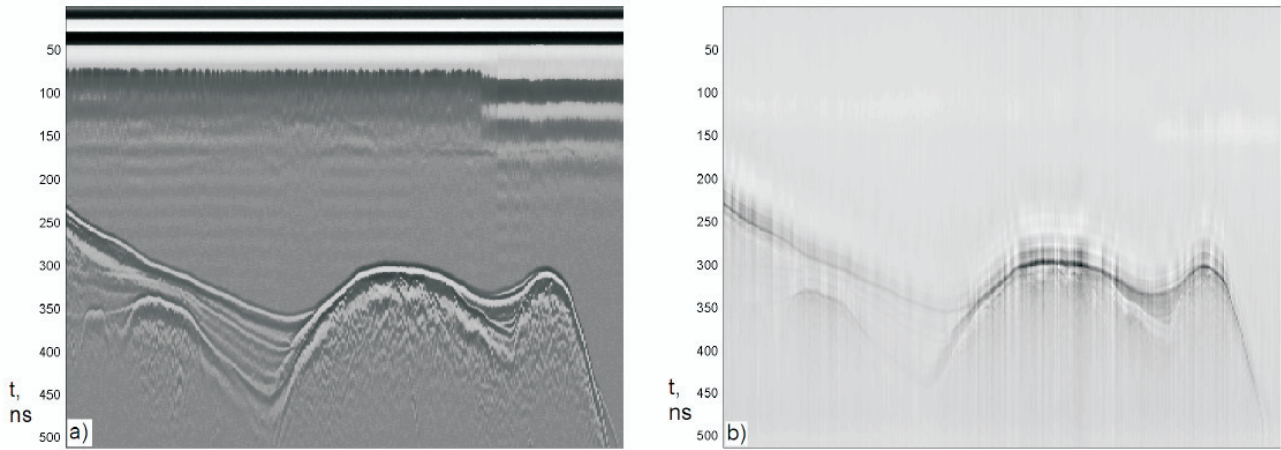
Fig. 6.   Example of real GPR common-offset data processing (lake bottom): a) raw data, b) after deconvolution.

and of the time-domain Green function are proportional to the current pulse image:

$$E^{\%}(r, \theta, p) = J^{\%}(p) G^{\%}(r, \theta, p) \qquad (20)$$

we can eliminate $J^{\%}(p)$ and obtain the following spectral relation

$$G^{\%}(p, x) = \frac{G_0^{\%}(p)}{E_0^{\%}(p)} E^{\%}(p, x) \qquad (21)$$

between the global wave field $E(r, \theta, t)$ and the field strength $E_0(t) = E(r_0, \theta_0, t)$ measured at an arbitrary chosen reference point (r_0, θ_0). By choosing $r_0 = 1$, $\theta_0 = \dfrac{\pi}{2}$, where ℓ is distance between the transmitter and receiver antennas, we can apply formula (21) to the common-offset scheme of GPR measurements ("B-scan") [11]:

$$G^{\%}(p, x) = \frac{G_0^{\%}}{E_0^{\%}(p)} E^{\%}(p, x) \qquad (22)$$

Here, $E^{\%}(p, x)$ is the actual GPR profile spectrum, $E_0^{\%}(p)$ – transformed waveform of the surface wave, $G_0^{\%}$ is the analytical function (15) calculated for $r = 1$, and $G^{\%}(p, x)$ is the Laplace spectrum of a virtual profile corresponding to a Heaviside step current. Inverse Laplace transform yields a rectified image of subsurface objects. As an example, in Fig.6(a) an experimental B-scan of a lake bottom, taken from the water surface, is depicted. Two distinct interfaces (bedrock and deposition) are blurred with phantom stratification caused by the probing pulse oscillations. The direct wave propagating along the water surface produces sharp stripes in the upper part of the profile.

A virtual "Heaviside" scan, with the direct wave and the probing pulse filtered out, is shown in Fig.6(b). Spurious strata being removed and real interfaces emphasized, this picture gives a more realistic view of the lake bottom shape and the underlying structures.

REFERENCES

[1] A. Sommerfeld, "Uber die Ausbreitung der Wellen in der Drahtlosen Telegraphie," *Annalen der Physik*, vol. 333, no. 4, pp. 665–736, 1909.
[2] V. A. Fock, "On Calculation of Electromagnetic Field of the Alternate Current Near a Plane Boundary," *Annalen der Physik*, vol. 17, no. 4, pp. 401–420, 1933.
[3] N. Engheta, C. H. Papas, and C. Elachi, "Interface Extinction and Subsurface Leaking of the Radiation Pattern of a Line Source," *Applied Physics*, vol. B26, no. 4, pp. 231–238, 1982.
[4] L. M. Brekhovskikh, *Waves in Layered Media*.   Academic Press, 1980.
[5] V. I. Smirnov, *A Course of Higher Mathematics*.   Oxford: Pargamon Press, 1964, vol. 3, Part 2.
[6] L. P. Zaitsev and N. V. Zvolinskiy, "Investigation of the Head Waves Generated at the Boundary Between Two Elastic Liquids," *Izvestiya Akademii Nauk SSSR, Seriya Geograficheskaya I Geofizicheskaya*, vol. 1, pp. 20–39, 1951, [In Russian].
[7] L. Crocco and F. Soldovieri, "From Qualitative to Quantitative Inverse Scattering Methods for GPR Imaging," in *Proceedings of 12th International Conference on Ground Penetrating Radar*, Birmingham, England, 2008.
[8] V. A. Borovikov, *Diffraction on Polygons and Polyhedra*.   Moscow: Nauka, 1966, [In Russian].
[9] E. A. Rudenchik, L. B. Volkomirskaya, A. E. Reznikov, and E. G. Bezrukova, "Analytical Representation of the Surface Wave Generated by Antenna at the Interface Between Two Homogeneous Media," *Physics of Wave Phenomena*, vol. 18, no. 2, pp. 1–9, 2010.
[10] I. S. Gradstein and I. H. Ryshik, *Table of Series, Products and Integrals*. Harri Deutsch Verlag, 1981.
[11] D. Daniels, *Ground-Penetrating Radar*.   London: IET, 2004.